

Three-dimensional simulation of detonation initiation and propagation in supersonic combustible mixtures

Xiaodong Cai¹, Jianhan Liang^{1*}, Yonggang Che², Ralf Deiterding³,
Zhiyong Lin¹ & Fengchen Zhuang⁴

¹Science and Technology on Scramjet Laboratory,

National University of Defense Technology, Hunan Changsha, 410073, China

²Science and Technology on Parallel and Distributed Processing Laboratory,

National University of Defense Technology, Hunan Changsha, 410073, China

³Institute of Aerodynamics and Flow Technology, German Aerospace Center(DLR),
Bunsenstr. 10, 37073, Göttingen, Germany

⁴The Academy of Equipment, Huairou, Beijing, 101416, China

Abstract: Detonation initiation and propagation in supersonic combustible mixtures using a hot jet have been investigated in three-dimensional numerical simulations with the detailed reaction model on Tianhe-2 system. Results indicate that the side walls can help realize the triple lines collisions and triple lines reflections, which play an important role in the detonation initiation. There should exist a critical width between the front and back sides of the three-dimensional channel for the successful initiation, which is totally different from that of two-dimensional cases. When the width exceeds the critical value, there will be not the effective reflections of the bow shock surface on the side walls, hence resulting in the failure of detonation initiation. For the detonation propagation, none of the standard detonation modes (rectangular mode, diagonal mode and spinning mode) is observed in the three-dimensional case. The initiated detonation is actually in an overdriven state because of the presence of the hot jet in the supersonic flow field, thus resulting in more complex detonation fronts than that in the CJ detonation. Because of both directions of three-dimensional detonation development than that of the two-dimensional case where the transverse waves propagation and the collisions of triple points can be realized only in one direction, the detonation fronts in three-dimensional simulation shows significantly larger irregularities and variations.

Keywords: Detonation Initiation and Propagation, Three-dimensional Simulation, Supersonic Combustible Mixtures, Hot Jet.

1 Introduction

Scramjets have become one of the first choices for hypersonic air-breathing propulsion systems due to the superior performance when the Mach number is above 5[1], but the practical applicability is still limited because of low net thrust. Scramjet combustors adopt the Brayton circle design whose thermodynamic efficiency(27%) is far below than that(49%) in the detonation combustion[2]. In principle, detonation based engine will be a promising one of the future propulsion systems with supersonic cruise velocity.

Because of their inherent theoretical advantage over deflagrative combustion, detonation combustion has been explored extensively for propulsion applications. In the detonation research, detonation initiation has

*Corresponding author's email: jhleon@vip.sina.com. This work is supported by National Natural Science Foundation of China No. 91016028 and Innovative Sustentation Fund for Excellent Ph.D. Students in NUDT No. B140101.

always been one of the key problems, especially in the supersonic combustible mixtures. Apart from direct initiations, an alternative initiation approach is the hot jet with active chemical, which can also achieve initiation very quickly[3]. Detonation initiation using a hot jet has been investigated in numerous studies in quiescent or low speed combustible mixtures[4, 5, 6, 7, 8, 9, 10, 11, 12], but rather few studies have been carried out in supersonic combustible mixtures. Ishii et al.[13] studied detonation initiation and propagation experimentally using a hot jet in combustible mixtures whose Mach number was 0.9 and 1.2. Xu Han et al.[14, 15] conducted experimental investigations of detonation initiation and the DDT(Deflagration to Detonation Transition) process induced by a hot jet in supersonic premixed flows. Their results confirm that a hot jet can initiate detonation combustion in supersonic combustible mixtures.

Experimental observations can provide only limited insight, and an alternative to laboratory experiments is numerical simulations. For detonation combustion calculations, chemical reaction generally introduces additional temporal and spatial scales. The reactive case generally requires finer meshes than studies of non-reactive Euler equations alone. However, only a small area near the detonation front, where there are severe chemical reactions, is in need of a very fine mesh while other areas with relatively mild flow behavior could be resolved with much coarser grid.

Here dynamic adaptive mesh refinement method is employed in order to decrease the computational costs while greatly improving the local resolution. Initially based on the DAGH software, the open-code program AMROC(Adaptive Mesh Refinement Object-oriented C++)[16] currently supports several Euler solvers for gas mixtures with complex equation of state, based on TVD and WENO schemes which is a sophisticated code that can be run on parallel computational platforms. A rigorous domain decomposition approach is used in the parallel implementation[17] that satisfies most of the partitioning objectives, except for some minor compromises. AMROC has been verified and demonstrated for multi-dimensional detonation combustions in numerous papers[16, 18, 19].

In our recent work[20, 21], through high-resolution two-dimensional simulations the mechanism for detonation initiation was explored and the effects of correlative geometrical parameters on detonation initiation were investigated using a hot jet in supersonic combustible mixtures with the simplified five-step chemical model[22] by applying AMROC. However, as the physical process taking place in detonation combustion is unsteady and essentially three-dimensional, there are limitations and difficulties in interpretation and understanding of the detonation physics from purely two-dimensional simulations. While there are undoubted similarities to some extent between two-dimensional numerical simulations and experimental researches for detonation initiation and propagation using a hot jet in supersonic combustible mixtures[23], the behavior of the flow can best be analyzed can explained with three-dimensional calculations. For three-dimensional simulations of detonation combustion, the simple chemical reaction models are usually utilized in order to decrease the computation cost[24, 25, 26, 27, 28, 29, 30]. Nevertheless, the simple reaction model utilized may have led to the loss of some fine features usually characterized by the complex chain-branching reaction process. Therefore, a detailed chemical model is needed to clarify and resolve the structure configuration and its evolution behavior.

Following the previous study, we have adopted AMROC for three-dimensional numerical simulations of detonation initiation and propagation in supersonic combustible mixtures with the detailed reaction model[31] on a nested parallel Linux compute platform. This reaction model consists of 9 species H_2 , H , O , O_2 , OH , H_2O , HO_2 , H_2O_2 , Ar and 34 elementary reactions, extracted from the larger hydrocarbon mechanism assembled by Westbrook.

2 Problem Statement

2.1 Calculation Model

The three-dimensional numerical simulations of detonation initiation and propagation in supersonic combustible mixtures with a hot jet are conducted in a rectangular channel, as depicted in Figure 1. Reflecting boundary conditions are imposed on the four walls, and a circular inflow of hot jet with a diameter D_j is embedded into the lower boundary. The right boundary models the inflow condition and the left one ideal outflow condition. Self-sustaining CJ detonations of H_2/O_2 mixtures in low pressure with high-argon dilution are ideal candidates for the numerical simulations of detonation initiation and propagation in supersonic combustibles, for very regular detonation cell patterns can be generated[32]. The rectangular channel consists

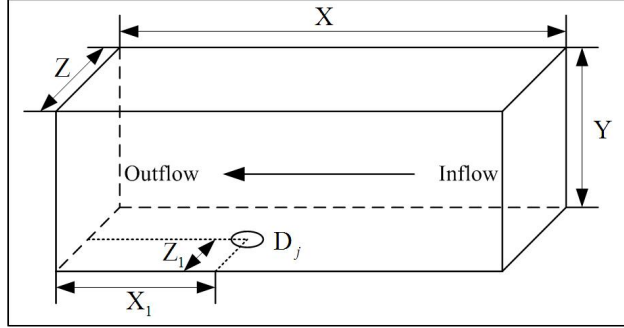


Figure 1: Schematic of calculation model.

Table 1: The equilibrium CJ state of H_2 and O_2 with a molar ratio of 2:1, 298K, 10kPa. Note that the parameters for the nine species are given the mass fractions

Parameters	Values
Pressure(Pa)	1.72718×10^5
Temperature(K)	3269.0376
Density(kg/m^3)	0.08972
Velocity(m/s)	1501.0624
Energy(J/m^3)	1.59548×10^5
H_2	2.40776×10^{-2}
H	7.59518×10^{-3}
O	5.3242×10^{-2}
O_2	1.21585×10^{-1}
OH	1.625166×10^{-1}
H_2O	6.30832×10^{-1}
HO_2	1.41912×10^{-4}
H_2O_2	9.15873×10^{-6}
Ar	0

of H_2 , O_2 , Ar mixtures with the molar ratio 2:1:7 under the condition of pressure 10kPa and temperature 298K, which flow at the velocity of $V_{CJ}=1627m/s$.

It is much more difficult for three-dimensional detonation initiations using a hot jet in supersonic combustible mixtures than that in two-dimensional detonation initiations, because in the two-dimensional detonation initiations, the hot jet actually blocks the whole flow in the real three-dimensional conditions. Here, we set the jet inflow parameters to the equilibrium CJ state of H_2 and O_2 with a molar ratio of 2:1 under the condition of the pressure 10kPa and the temperature 298K, calculated from Cantera[33], as shown in Table 1. In order to produce a strong hot jet, the velocity is given the sound speed for the equilibrium state to make it a choked hot jet.

2.2 Numerical Scheme

The detonation initiation and propagation in supersonic combustible mixtures is modeled using the three-dimensional Euler equations for a mixture of different thermally perfect species with chemically reactive source terms[16]. A second-order accurate MUSCL-TVD finite volume method(FVM) is adopted for convective flux discretization. The hydrodynamic solution process in AMROC is divided into two steps: the numerical flux calculation step and the reconstruction step. In the reconstruction step, linear interpolation is used to construct interfacial values from cell-centered one. Limiter functions prevent oscillations at discontinuities to satisfy the properties of a TVD scheme. The constructed neighboring values are then used in the calculation step to approximate the average flux on the element interfaces by an upwind scheme.

Dimensional splitting is employed for the three-dimensional numerical simulations. Since the differences between considering the reaction source term with first-order accurate Godunov splitting or with second-order accurate Strang splitting are usually small[16], we have adopted the computationally more efficient Godunov splitting method here. A hybrid Roe-HLL[16] Riemann solver is used to construct the inter-cell numerical upwind fluxes; the Van Albada limiter with MUSCL reconstruction is applied to construct a second-order method in space. The MUSCL-Hancock technique[34] is adopted for second-order accurate time integration, and all simulations use dynamic time step adjustment with the target CFL number 0.95.

3 Results and Discussions

As shown in Figure 1, the length of the rectangular channel is $X=3.2\text{cm}$, the height is $Y=1.6\text{cm}$, and the width is $Z=0.8\text{cm}$. The diameter of the hot jet is $D_j=4.0\text{mm}$, and $X_1=1.2\text{cm}$, $Z_1=0.5Z=0.4\text{cm}$. The base grid is $64 \times 32 \times 16$. The detonation cell size under these conditions is $\lambda=1.6\text{cm}$, so the setup allows the development of a full detonation cell in the Y direction. The three-dimensional computations were run on Tianhe-2 system in Guangzhou city with 1024 Intel E5-2629 2.20 GHz(Ivy Bridge) processors.

3.1 Verification of Adaptive Mesh Refinement

It is found that for the detailed reaction considered here, a spatial resolution of minimally $6Pts/l_{ig}$ is necessary to resolve all intermediate reaction products in the one-dimensional ZND solution accurately[35]. Around multi-dimensional triple points, a higher resolution is required to capture the internal wave structure completely. The previous three-dimensional verification simulation[18] for the regularly oscillating case uses effective resolution up to $16.8Pts/l_{ig}$, whose adaptive results are in perfect agreement with the calculations by Tsuboi et al.[36] for the same configuration obtained on a uniform mesh on a superscalar vector machine. In order to accommodate a reduction of the induction length when the detonation gets overdriven by the ejection of the hot jet[20], the computations here use an effective resolution of $30.85Pts/l_{ig}$, which is achieved by five-level mesh adaptation with refinement factors 2, 2, 2, 2. A physically motivated combination of scaled gradients of pressure, density and temperature and heuristically estimated relative errors in the mass fractions is applied as adaptation criteria[16]. For SAMR(Structured Adaptive Mesh Refinement) grid generation, a flagging efficiency value of 0.9 is used, where flagging efficiency is the ratio between flagged cells and all cells in every new sub-grid[37].

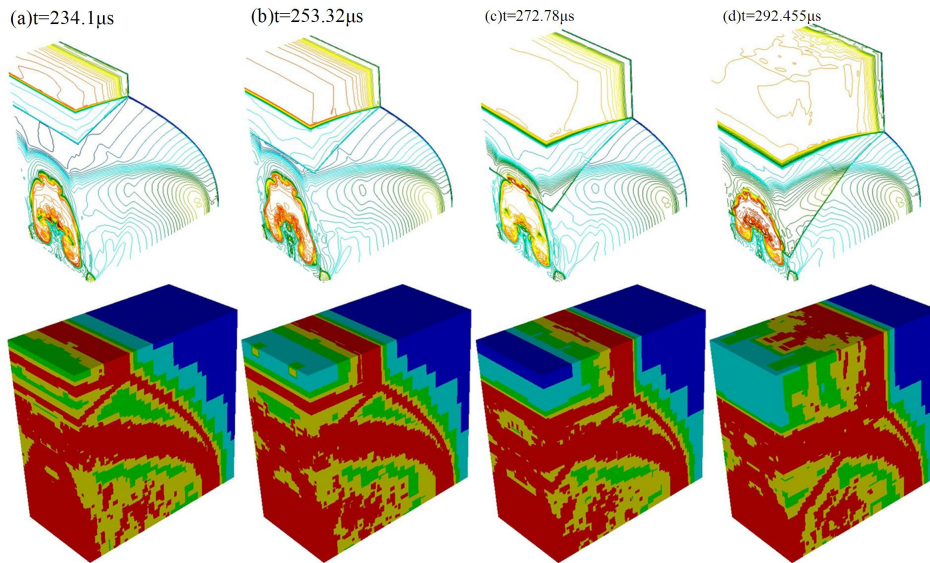


Figure 2: Temperature contours(upper) and the corresponding adaptive level distributions(lower). The mesh adaptation is five-level refinement represented by five different colors. The red color shows the highest fifth refinement level, and the blue color shows the base level.

Figure 2 visualizes temperature contours and the corresponding adaptive level distributions at four different times. In Figure 2(a), a mach stem is formed after the reflection on the upper wall of the bow shock induced by the hot jet. It is clearly shown that in the structure of the triple line, there consist of the incident shock wave(the bow shock induced by the hot jet), the Mach stem and the transverse wave(the reflection wave) along with a slip surface behind the triple line. In addition, behind the bow shock surface, there is a combustion surface decoupled with the bow shock. All the features, including the structure of triple line and the combustion surface behind the bow shock, are all resolved with the highest refinement level. In Figure 2(b), the Mach stem propagates forward along the bow shock and becomes longer. It is clearly suggested that the dynamic adaptive mesh in the corresponding level distribution has captured precisely the change of the flow. In Figure 2(c), with the further propagation, the flow behind the Mach stem becomes milder shown in the temperature contour, and the refinement level becomes coarser to reduce the computational cost. However, in Figure 2(d), the Mach stem becomes unstable resulting in the perturbation behind the Mach stem. Hence, the course mesh in Figure 2(c) is refined again to adapt the new change.

In this case, high resolution in these areas where the scaled gradients or heuristically estimated relative errors are large is achieved while other areas are resolved coarser. It is imminent that the mesh adaption flag parameters perform satisfactorily for the cases. In this way, the high-resolution calculation efficiency is improved by decreasing the computation cost.

3.2 Detonation Initiation

The three-dimensional detonation initiation process in supersonic combustible mixtures using a hot jet is shown in Figure 3. After the sonic ejection of hot jet into the rectangular channel, a bow shock surface is induced by the hot jet in the supersonic flow. This shock surface spreads from the middle to both sides. The shock surface is strongest in the middle line, while it decreases when spreading out to the both sides. During a period of time, the bow shock surface becomes stronger as a whole, and the side shock waves realize the first reflection on the side walls, as shown in Figure 3(a). The reflections on the side walls can enhance the strength of the bow shock surface at the same time, hence the bow shock surface can rise more quickly to reflect on the upper wall and finally a Mach stem is formed on the upper wall, as shown in Figure 3(b).

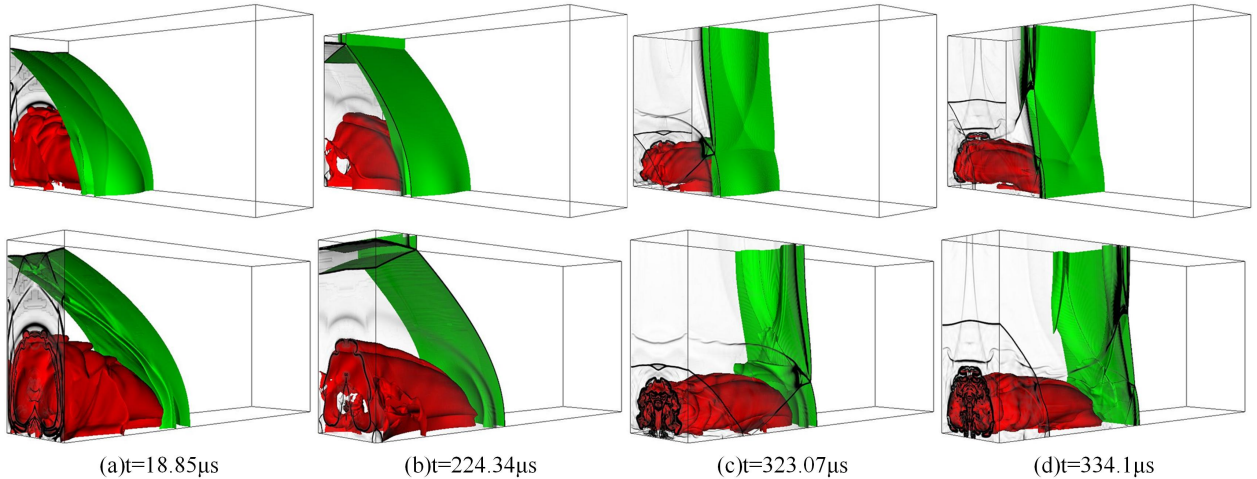


Figure 3: Front(upper) and rear(lower) view of density isofaces and numerical schlieren images showing the initiation process using a hot jet in the three-dimensional channel. The green density isoface is at the density of $0.3\text{kg}/\text{m}^3$.

The detailed structure of the Mach stem can be seen in Figure 4. The OH mass fraction images in Fig.4 show that there exists a combustion zone behind the Mach stem. Indicated by the distance between the OH front and Mach stem (presented by the density isoface), the combustion front is tightly coupled with the Mach stem. In the numerical schlieren images, it can be obtained that the distance is $l = 0.715\text{mm}$, only about three quarters of the theory ZND induction length l_{ig} ($l_{ig} = 0.964\text{mm}$). From the comparison

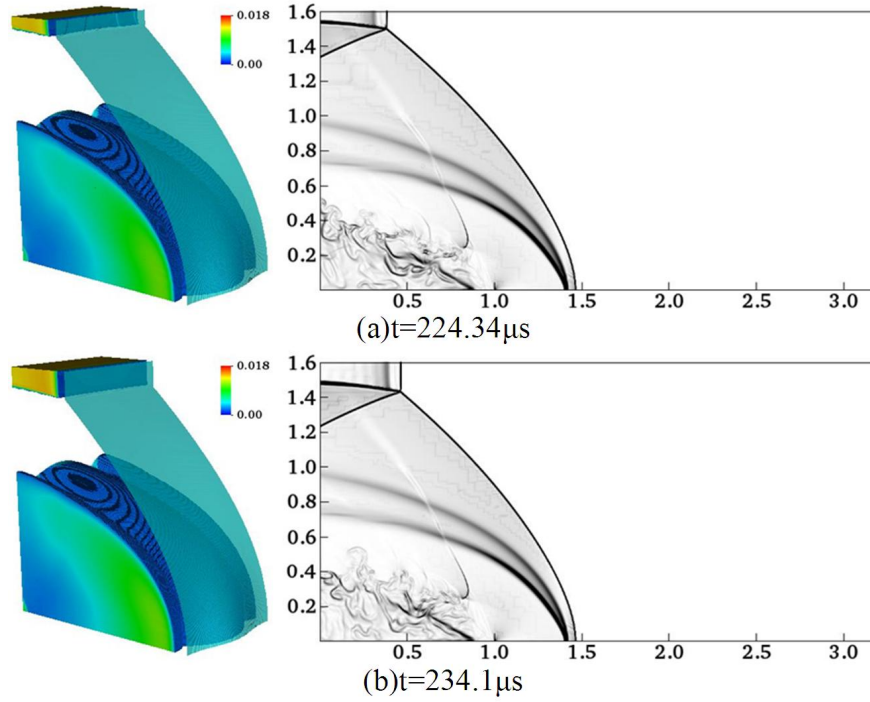


Figure 4: The OH mass fraction pseudocolors and the density isofaces(left) and the numerical schlieren images vertical to Z direction in the channel center(right). The light blue density isoface is at the density of $0.3\text{kg}/\text{m}^3$.

between Figure 4(a) and Figure 4(b), the Mach stem can propagate forward when the supersonic incoming flow enters at V_{CJ} . It is indicated that the Mach stem is actually a locally overdriven detonation.

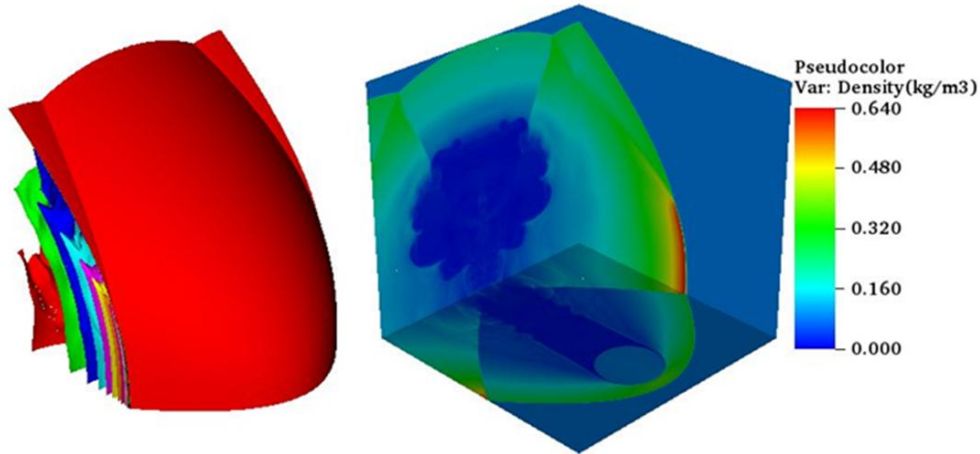


Figure 5: The temperature isoface and the density pseudocolor showing the stable bow shock surface when $Z=1.6\text{cm}$.

The Mach stem in Figure 3(c) has propagated forward obviously, and at the same time the triple lines produced by the reflections on the side walls collide together in the horizontal direction. It is shown in Figure 3(c) that a prominent cambered shock surface is generated because of the instantaneous strong heat release after the triple line collision. The Mach stem continues the propagation and finally realizes the first reflection on the lower wall along with the triple lines reflections on the side walls, as shown in Figure 3(d). It can be

concluded that during the three-dimensional detonation initiation, the triple lines collisions and triple lines reflections on the surrounding four walls in the channel play an important role on the successful initiation. The triple lines collisions and triple lines reflections can both release strong chemical energy instantaneously as the local ignition source, thus resulting in the continuous detonation initiation in the whole channel.

When the width of the channel is increased to $Z=1.6\text{cm}$ and the hot jet is still located in the middle of the channel while the other conditions are kept the same, the induced bow shock surface is shown in Figure 5. When the shock surface spreads out to the both sides, it gets weaker because of the larger width. Although the strength of the wave becomes larger to some degree after the reflections on the side wall as shown from the temperature isoface in Figure 5, it is still not strong enough to enhance the bow shock surface to realize the effective reflection on the upper wall. Finally, detonation initiation is not realized successfully, and the flow field keeps the stable structure of bow shock surface reflection induced by the hot jet.

In the two-dimensional simulations of detonation initiation, the hot jet actually blocks the whole flow in the real three-dimensional conditions. The bow shock induced by the hot jet will not spread out to the both sides and can maintain the same strength. Nevertheless, the two-dimensional detonation initiation still cannot be realized, and the flow field maintains the stable induced shock wave, as shown in Figure 6(a). When the hot jet is newly located at $[1.5, 1.9]\text{cm}$, as shown in Figure 6(b), a shock wave reflection is formed on the upper wall, but the initiation is still not realized eventually and the flow field maintains the stable shock wave reflection all the way.

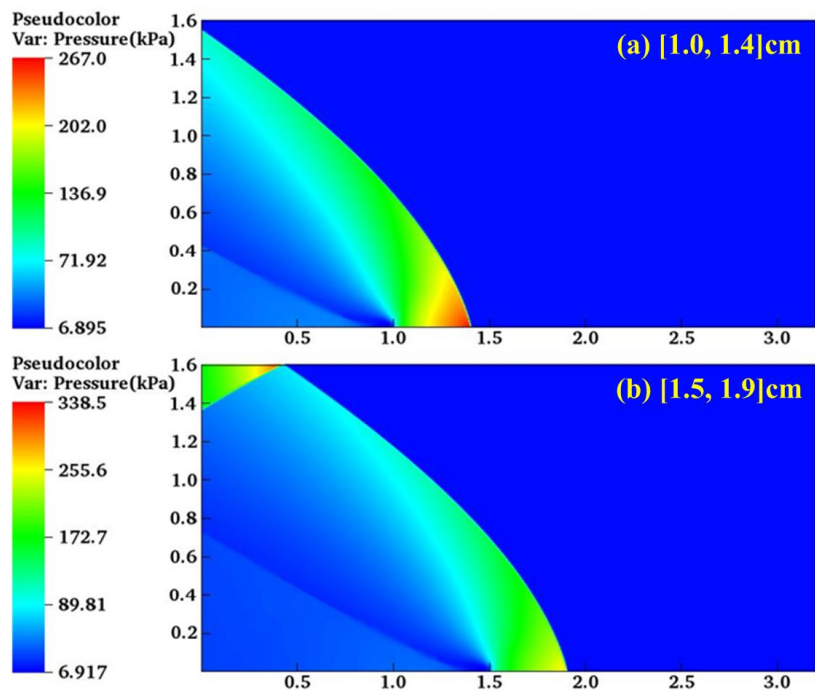


Figure 6: Two-dimensional induced shock reflections for two different locations of hot jet.

It is suggested that in the three-dimensional simulation, the side walls help realize the triple lines collisions and triple lines reflections which play an important role in the detonation initiation in supersonic combustible mixtures using a hot jet, which is different from two-dimensional cases. For certain conditions, there should exist a critical distance between the both sides of the channel for the successful initiation. When the distance exceeds the critical value, there will be not the effective reflection of bow shock surface on the side walls, hence resulting in the failure of detonation initiation.

3.3 Detonation Propagation

After the successful initiation, the initial transverse wave surface propagates between the upper wall and the lower wall until the complete detonation combustion is formed in the entire channel. With the continuous

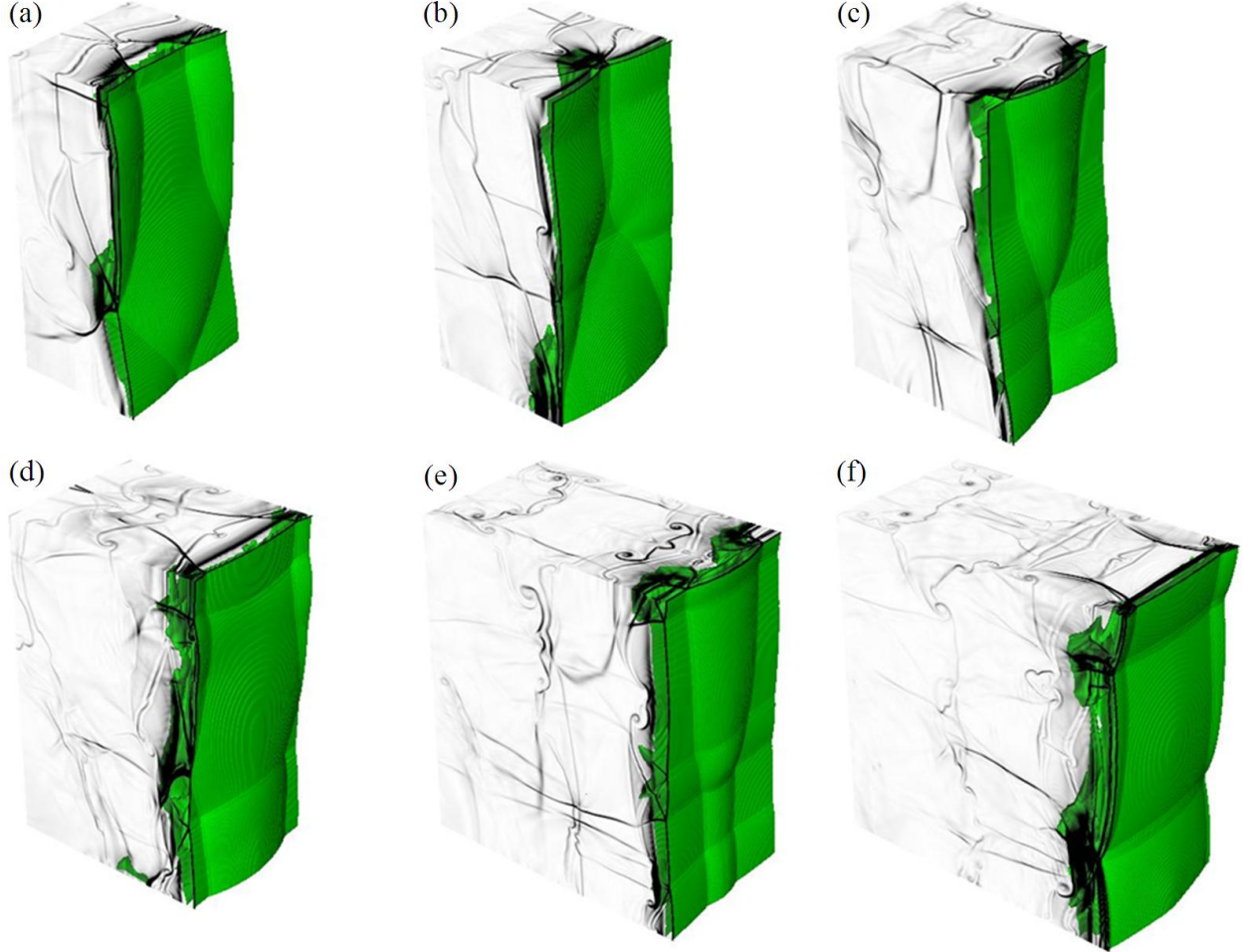


Figure 7: The development of overdriven detonation shown by the density isofaces and numerical schlieren images.

ejection of the hot jet, the detonation wave can keep on propagating forward in the supersonic incoming flow with V_{CJ} , indicating that the detonation wave is actually in an overdriven state.

The overdriven detonation is essentially unstable, which is shown in Figure 7. In Figure 7(a), two groups of triple lines are generated. The group of triple lines on the upper part are beginning the collision each other. The other group of triple lines on the lower part travel in an opposite direction and will reflect on the side walls. In Figure 7(b), the two groups of triple lines both realize the collision or reflection. The collisions or reflections of the two triple lines can instantly produce areas of high temperature and pressure as strong initiation sources, resulting in the formation of locally overdriven detonations, as shown in Figure 7(c). Subsequently, the reflections on the front and back walls also generate new transverse wave surfaces and triple lines. The new triple lines propagate between the front and back walls, and finally also form the collisions, generating a newly overdriven detonation in the Z direction. Gradually, more transverse wave surfaces and triple lines are generated in the overdriven detonation because of the essential instability, as shown from Figure 7(d) to Figure 7(f). Figure 8 visualizes the numerical schlieren profiles at nine different locations in the X directions. It is shown that the flow field changes quite a lot in different locations. The propagation of the transverse wave surfaces and the collisions of the triple lines between both Y and Z directions generally result in the complex structures of three-dimensional overdriven detonations.

In the previous three-dimensional detonation simulations in rectangular channels with simplified reaction models or detailed reaction models, the results show the presence of a rectangular mode, a diagonal mode or even a spinning mode of the detonation front[24, 26, 28, 29, 38]. However, in the simulation here, none of these

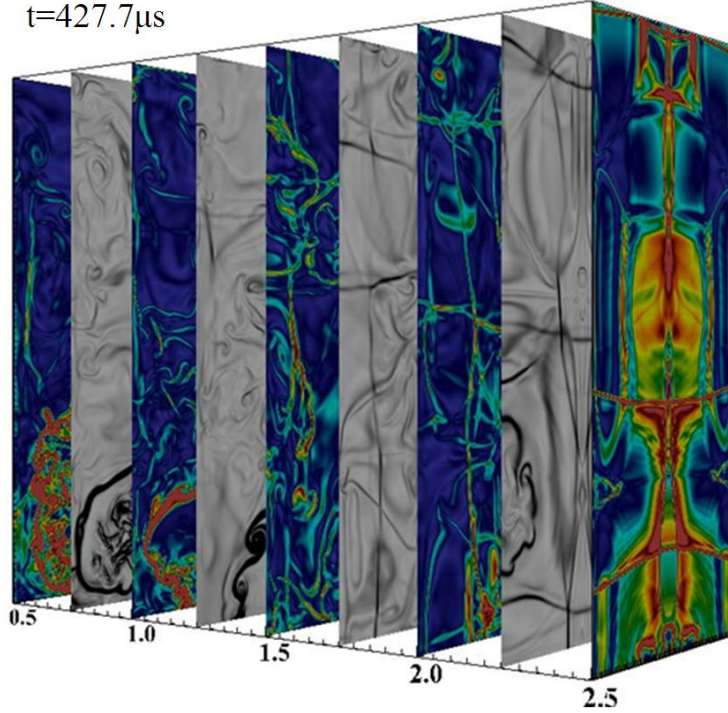


Figure 8: The numerical schlieren profiles at nine locations when $t=427.7\mu s$.

standard detonation modes is observed. For the previous investigations of three-dimensional simulations, the ZND solution is usually used as the initial condition and the CJ detonation can be obtained directly, ignoring totally the overdriven state. Nevertheless, because of the presence of the hot jet in the flow field, the initiated detonation in supersonic combustible mixtures is actually in an overdriven state[20], thus resulting in more complex three-dimensional detonation fronts than the CJ detonation. Unlike Williams et al.[39] who presented a similar simulation for an overdriven detonation, no phaseshift is observed between both Y and Z directions here. A simplified one-step reaction model is used in that simulation, but it may result in inaccuracy because certain features in detonation combustions are characterized mainly by the detailed chain-branching reactions.

Figure 9 shows the combustion fronts (represented by the OH mass fractions pseudocolors) overlaid by the detonation fronts (represented by the light blue density isofaces), which visualizes the induction length of the overdriven detonation. In Figure 10, the variation of the induction length is clearly visualized through three frames when projecting the three-dimensional flow field to two-dimensional images. The corresponding two-dimensional simulation realizing the successful detonation initiation is conducted at the same time using a stronger hot jet. The stronger hot jet pressure is 1.2 times of that in the CJ state, and the other conditions all maintain the same. Its overdriven state is shown in Figure 11 with the numerical schlieren images. Indicated by the four frames in Figure 11, the induction length in the two-dimensional case almost keeps the same value of 0.7mm, approximately equal to that in Figure 4. Compared with the two-dimensional case in Figure 11, however, the induction length in three-dimensional simulation shows significantly larger irregularities and variations than that in the two-dimensional case, indicating that the detonation front is more complex in the three-dimensional case because of both directions of detonation development than that in the two-dimensional one where the propagation transverse waves and the collision of triple points can be realized only in one direction. However, the oscillation period is almost identical in both two and three-dimensional cases, indicating that the basic two-dimensional instability is preserved in three-dimensional simulations.

Figure 12(a) shows the location history of the shock front in the whole two-dimensional detonation initiation and propagation process. Before the hot jet is shut down, the location history curve is actually a straight line, showing that the detonation keeps an invariable overdriven degree with the continuous

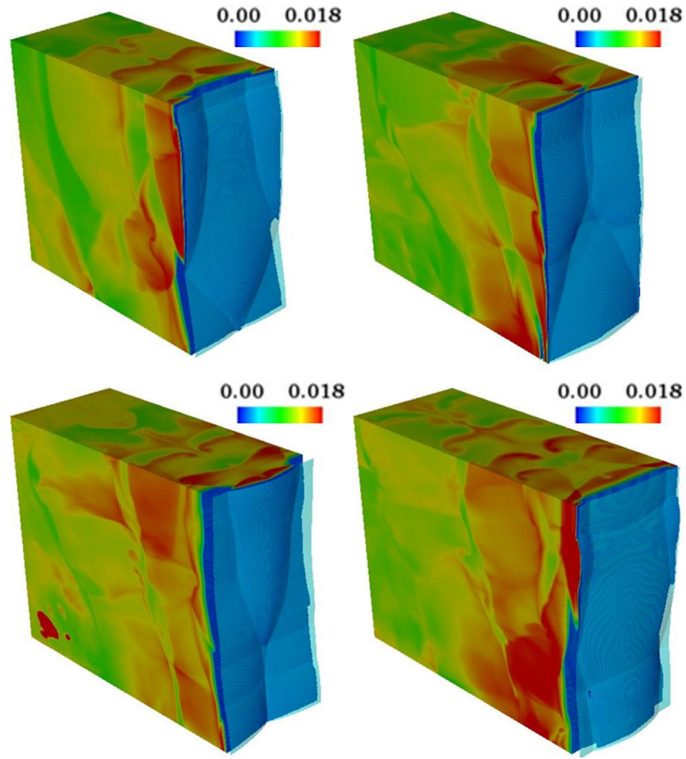


Figure 9: The structures of overdriven detonation front and the induction zone shown by the OH mass fraction pseudocolors and density isofaces at a density of 0.3kg/m^3 .

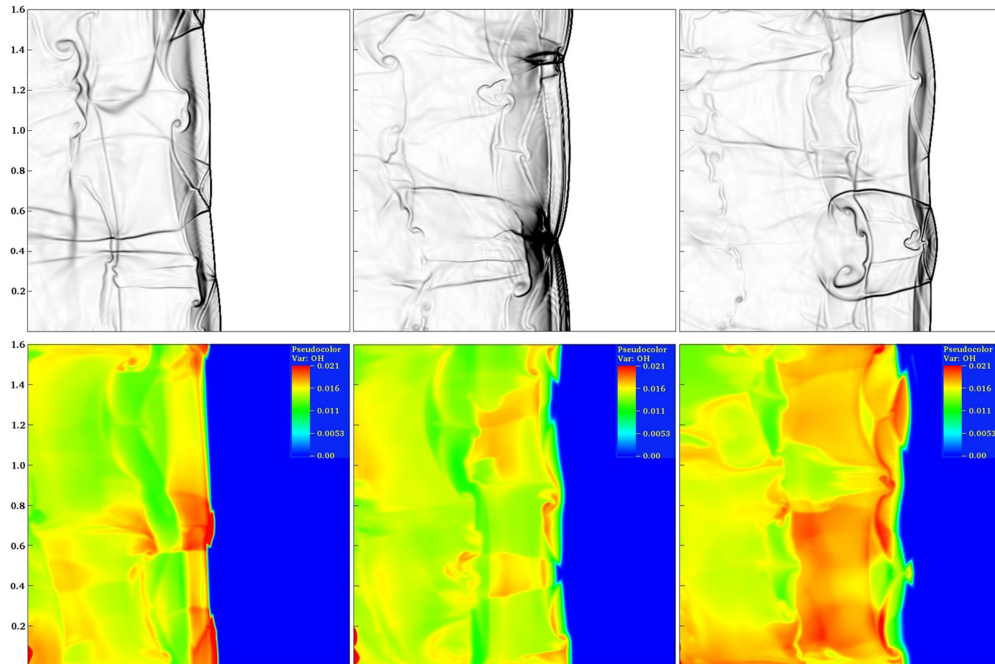


Figure 10: The numerical schlieren images(upper) and the corresponding OH mass fraction pseudocolors(lower) vertical to Z direction in the channel center.

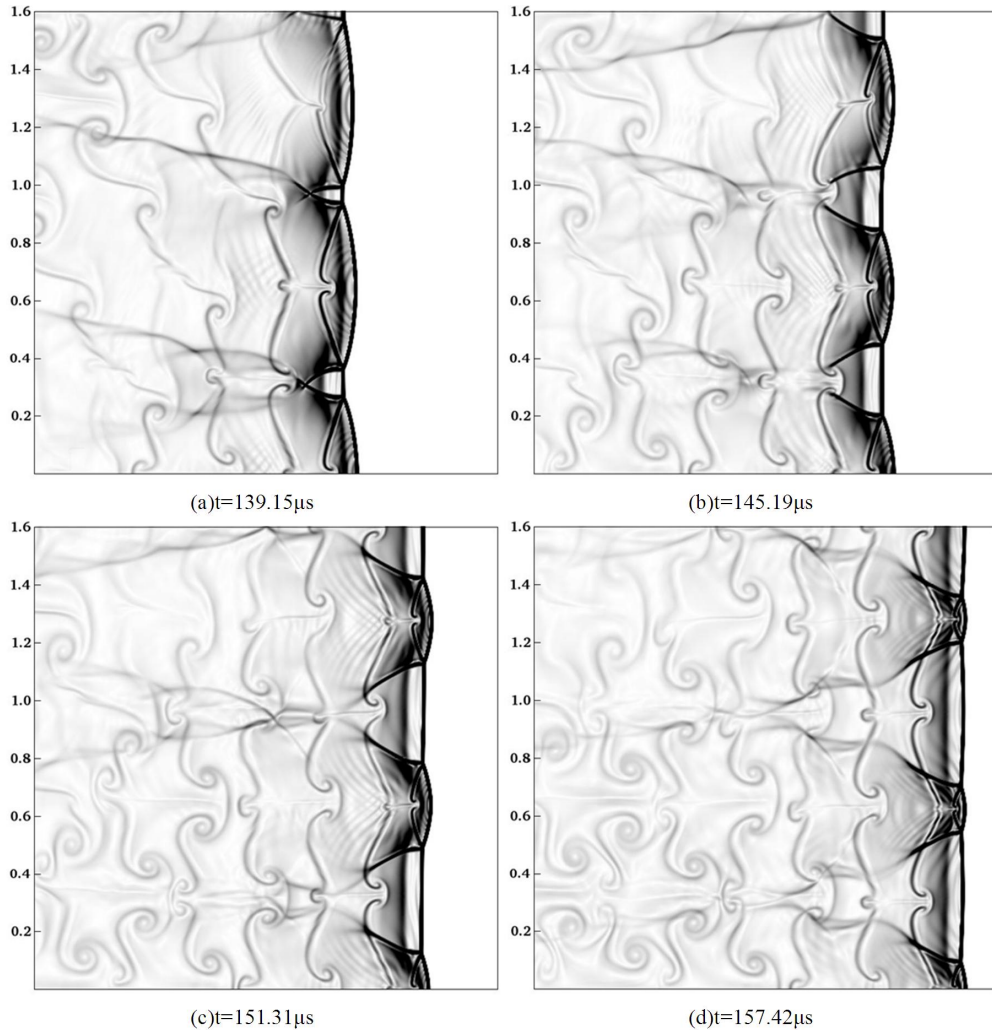


Figure 11: The numerical schlieren images showing the overdriven detonation propagation for the corresponding two-dimensional detonation initiated using a hot jet.

ejection of hot jet. In Figure 7, it is suggested that an invariable overdriven degree is also obtained in the three-dimensional case. However, the overdriven degrees are different values in the two cases because of the different hot jet and dimensional setups. After the hot jet is shut down, the slope of the curve gradually decreases, meaning that the propagating velocity of the detonation wave slows down, indicating the detonation attenuation without the hot jet. The attenuation of the overdriven detonation gradually results in the weakening of the transverse wave surfaces. As a result, the small irregular detonation cells grow into large regular detonation cells until the formation of CJ detonation. At about $t=400\mu s$ as shown in Figure 12(b), the detonation front is kept almost at the same position, maintaining a relatively dynamic stability, indicating the eventual formation of the CJ detonation. Figure 12(b) shows the regularly periodic oscillation curve of the CJ detonation. The oscillation period can be calculated as about $\delta T = 18\mu s$. Therefore, the velocity of the transverse wave can be estimated as $v_t = \gamma/\delta T$, which is approximately equal to the local sonic speed behind the detonation front and in a good agreement with Lee[40]. The CJ detonation is shown in Figure 13 with the temperature and OH mass fractions pseudocolors. One regular detonation cell fills the channel, and a keystone-like feature is clearly visible in the OH mass fraction pseudocolor of Figure 13(a), which is quite similar with the result in Z. Liang et al.[22]

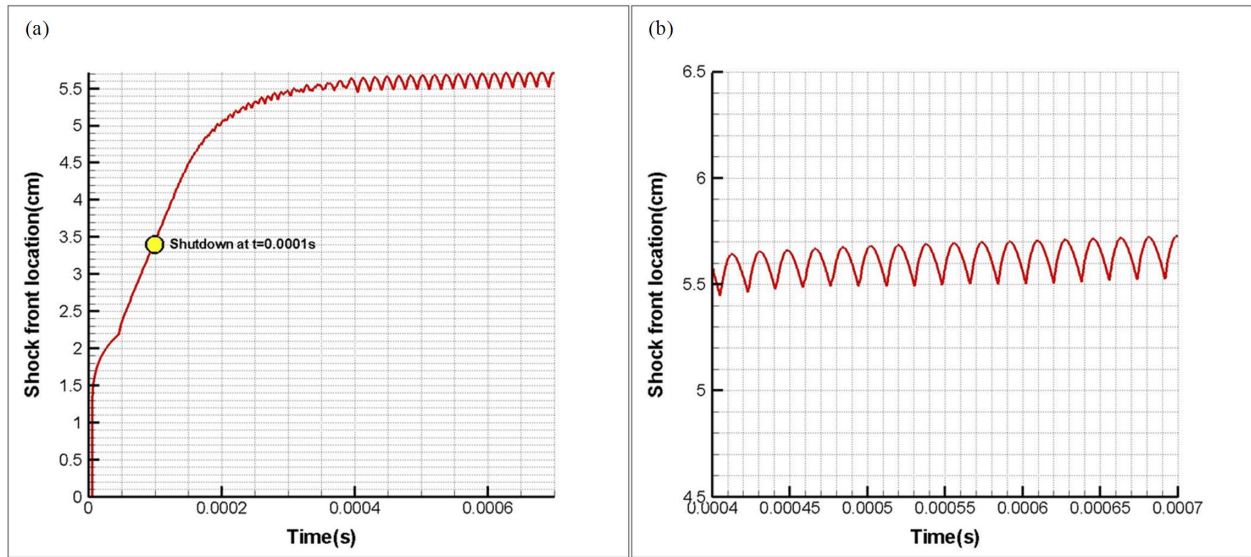


Figure 12: The entire location history of the shock front(left) and the oscillation location history of the CJ detonation after the shutdown of the hot jet(right).

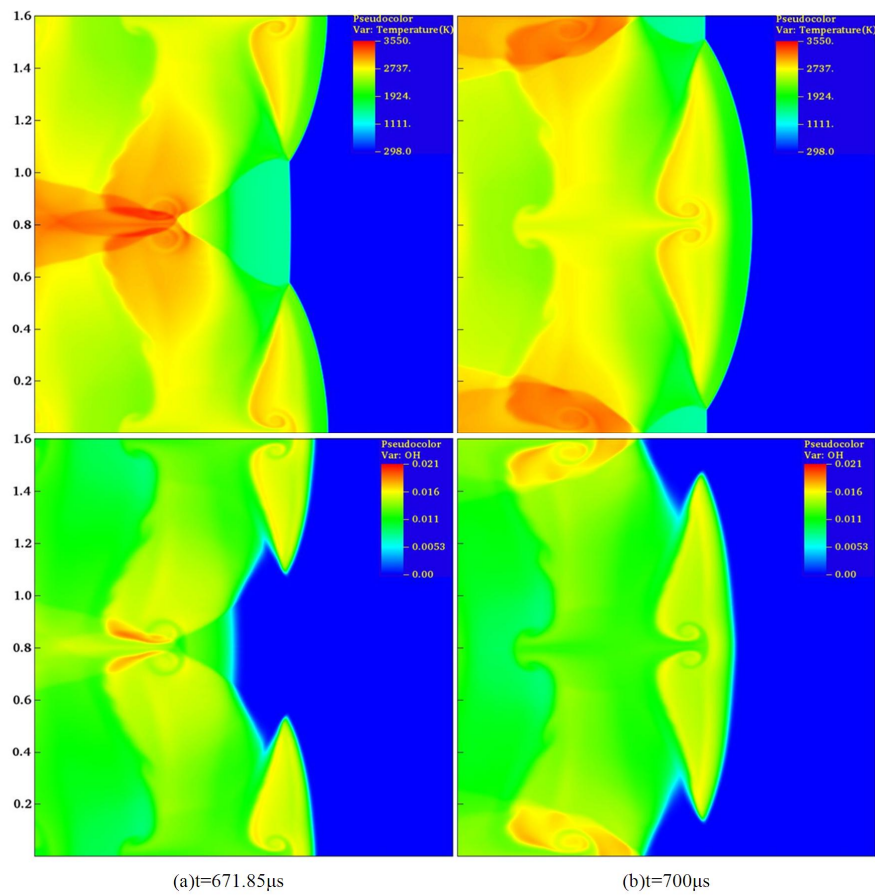


Figure 13: The CJ detonation for the two-dimensional case after the shutdown of the hot jet.

4 Conclusion and Future Work

Three-dimensional numerical simulations of detonation initiation and propagation using a hot jet in supersonic combustible mixtures have been investigated with the adaptive mesh refinement open-code program AMROC, and the detailed chemical reaction model is adopted in the simulations. The corresponding two-dimensional simulations are also conducted in order to better examine the actual physical process through the comparison.

Results indicate that in the three-dimensional simulation the side walls can help realize the triple lines collisions and triple lines reflections, which play an important role in the detonation initiation in supersonic combustible mixtures using a hot jet. For certain conditions, there should exist a critical width between the front and back sides of the three-dimensional channel for the successful initiation. When the width exceeds the critical value, there will be not the effective reflections of the bow shock surface on the side walls, hence resulting in the failure of detonation initiation. For the three-dimensional detonation propagation, none of the standard detonation modes (rectangular mode, diagonal mode and spinning mode) is observed. The initiated detonation is actually in an overdriven state because of the presence of the hot jet in the supersonic flow field, thus resulting in more complex detonation fronts than that in the CJ detonation. Because of both directions of three-dimensional detonation development than that of the two-dimensional one where the transverse waves propagation and the collisions of triple points can be realized only in one direction, the detonation fronts in three-dimensional simulation shows significantly larger irregularities and variations than that in the two-dimensional case.

It should be noted that the present simulations have some limitations. The computational domain is relatively smaller than the actually experimental domains because of the huge computational cost resulted from the high grid resolution and detailed reaction model. The three-dimensional detonation initiation and propagation are of interest, hence the viscous effects, such as turbulence and boundary layer interactions, are ignored in the simulations. However, although they may not affect the overall detonation structure[41], the viscous effects should be considered in the future work.

5 Acknowledgements

The authors thank the support from the Parallel Visualization Center in School of Computer in NUDT for the visualization of the three-dimensional large-scale data obtained from Tianhe-2 system in Guangzhou city.

References

- [1] Murthy S.N.B and Curran E.T. High-speed flight propulsion systems. *Progress in astronautics and aeronautics*, 137:124–158, 1991.
- [2] Kailasanath K. Review of propulsion applications of detonation waves. *AIAA Journal*, 38(9):1698–1708, 2000.
- [3] R. Knystautas J.H. Lee I. Moen and H.G.G. Wagner. Direct initiation of spherical detonation by a hot turbulent gas jet. *Seventeenth Symposium (International) on Combustion*, 17:1235–1245, 1979.
- [4] Moen I.O. Bjerketvedt D. Jenssen A. and Thibault P.A. Transition to Detonation in Large Fuel-Air Cloud. *Combustion and Flame*, 61:285–294, 1985.
- [5] F. Carnasciali J.H.S. Lee R. Knystautas and F. Fineschi. Turbulent Jet Initiation of Detonation. *Combustion and Flame*, 84:170–180, 1991.
- [6] Dorofeev S.B. Bezmelnitsin A.V. Sidorov V.P. Yankin J.G. and Matsukov I.D. Turbulent Jet Initiation of Detonation in Hydrogen-Air Mixtures. *Shock Waves*, 6:73–78, 1996.
- [7] Lieberman D.H. Parkin K.L. and Shepherd J.E. Detonation Initiation by a Hot Turbulent Jet for Use in Pulse Detonation Engines. *AIAA Paper 2002–3909*, 2002.
- [8] S.P. Medvedev S.V. Khomik H. Olivier A.N. Polenov A.M. Bartenev and B.E. Gelfand. Hydrogen detonation and fast deflagration triggered by a turbulent jet of combustion products. *Shock Waves*, 14:193–203, 2005.
- [9] John L. Hoke Royce P. Bradley Jason R. Gallia and Frederick R. Schauer. The Impact of Detonation Initiation Techniques on Thrust in a Pulsed Detonation Engine. *AIAA Paper 2006–1023*, 2006.

- [10] Shijie Liu Zhiyong Lin Weidong Liu Wei Lin and Fengchen Zhuang. Experimental Realization of H₂/Air Continuous Rotating Detonation in a Cylindrical Combustor. *Combustion Science and Technology*, 184:1302–1317, 2012.
- [11] Iglesias I. Vera M. Sánchez A. L. Liñán A. Numerical analyses of deflagration initiation by a hot jet. *Combustion Theory and Modelling*, 16:994–1010, 2012.
- [12] Xiaodong Cai Jianhan Liang Zhiyong Lin Xu Han Hui Qin. Numerical simulation of detonation initiation in quiescent combustible mixtures with block-structured adaptive mesh refinement method. *Journal of Propulsion Technology*, 35(2):236–243, 2014.
- [13] K. Ishii H. Kataoka T. Kojima. Initiation and propagation of detonation waves in combustible high speed flows. *Proceedings of Combustion Institute*, 32:2323–2330, 2009.
- [14] Han Xu Zhou Jin Lin Zhiyong. Experimental investigations of detonation initiation by hot jets in supersonic premixed flows. *Chin. Phys. B.*, 21:124702, 2012.
- [15] Han Xu Zhou Jin Lin Zhiyong Liu Yu. Deflagration-to-Detonation Transition Induced by Hot Jets in a Supersonic Premixed Airstream. *CHIN. PHYS. LETT.*, 30:054701, 2013.
- [16] R. Deiterding. Parallel adaptive simulation of multi-dimensional detonation structures. Ph.D. thesis, Brandenburgische Technische Universit at Cottbus, 2003.
- [17] R. Deiterding. *Construction and application of an AMR algorithm for distributed memory computers*. Springer, 2005.
- [18] Ralf Deiterding. High-Resolution Numerical Simulation and Analysis of Mach Reflection Structures in Detonation Waves in Low-Pressure H₂-O₂-Ar Mixtures: A Summary of Results Obtained with the Adaptive Mesh Refinement Framework AMROC. *Journal of combustion*, 2011, 2011.
- [19] Ralf Deiterding. A parallel adaptive method for simulating shock-induced combustion with detailed chemical kinetics in complex domains. *Computers and Structures*, 87:769–783, 2009.
- [20] Xiaodong Cai Jianhan Liang Zhiyong Lin Ralf Deiterding Hui Qin and Xu Han. Adaptive mesh refinement based numerical simulation of detonation initiation in supersonic combustible mixtures using a hot jet. *ASCE Journal of Aerospace Engineering*, 2013. DOI: 10.1061/(ASCE)AS. 1943-5525.0000376.
- [21] Xiaodong Cai Jianhan Liang Zhiyong Lin and Fengchen Zhuang. Influence analysis of geometrical parameters of detonation initiation with a hot jet by adaptive mesh refinement method. *AIAA Paper* 2013-4167, 2013.
- [22] Z. Liang S. Browne R. Deiterding and J.E. Shepherd. Detonation front structure and the competition for radicals. *Proceedings of Combustion Institute*, 31:2445–2453, 2007.
- [23] Xiaodong Cai Jianhan Liang Zhiyong Lin Ralf Deiterding and Yu Liu. Parametric study of detonation initiation using a hot jet in supersonic combustible mixtures. *Aerospace Science and Technology*, 2014. <http://dx.doi.org/10.1016/j.ast.2014.05.008>.
- [24] Vincent Deledicque and Miltiadis V. Papalexandris. Computational study of three-dimensional gaseous detonation structures. *Combustion and Flame*, 144:821–837, 2006.
- [25] Cheng Wang Jie Lu and Ting Ye. Numerical Simulation of Three-dimensional Gas Detonation. *Journal of Physics*, 96:012029, 2008.
- [26] HuaShu Dou Her Mann Tsai Boo Cheong Khoo and Jianxian Qiu. Simulations of detonation wave propagation in rectangular ducts using a three-dimensional WENO scheme. *Combustion and Flame*, 154:644–659, 2008.
- [27] Huang Yue Ji Hua Lien FueSang and Tang Hao. Three-Dimensional Parallel Simulation of Formation of Spinning Detonation in a Narrow Square Tube. *CHIN. PHYS. LETT.*, 29(11):114701, 2012.
- [28] Cheng Wang ChiWang Shu Wenhui Han and Jianguo Ning. High resolution WENO simulation of 3D detonation waves. *Combustion and Flame*, 160:447–462, 2013.
- [29] Deok-Rae Cho Su-Hee Won Jae-Ryul Shin and Jeong-Yeol Choi. Numerical study of three-dimensional detonation wave dynamics in a circular tube. *Proceedings of the Combustion Institute*, 34:1929–1937, 2013.
- [30] S.M. Frolov A.V. Dubrovskii and V.S. Ivanov. Three-dimensional numerical simulation of operation process in rotating detonation engine. *Progress in Propulsion Physics*, 4:467–488, 2013.
- [31] Charles K. Westbrook. H₂-O₂-AR Reaction Mechanism from: Chemical Kinetics of Hydrocarbon Oxidation in Gaseous Detonations. *Combustion and Flame*, 46:191–210, 1982.
- [32] Strehlow R.A. Gas phase detonations: Recent developments. *Combustion and Flame*, 12:81–101, 1968.
- [33] D. Goodwin. *Cantera: Object-Oriented Software for Reacting Flows*. Tech. Rep., California Institute

of Technology, <http://www.cantera.org>.

- [34] B. van Leer. On the relation between the upwind-differencing schemes of Godunov, Engquist-Osher and Roe. *SIAM J. Sci. Statist. Comput.*, 5:1–20, 1984.
- [35] R. Deiterding and G. Bader. *High-resolution simulation of detonations with detailed chemistry*. Springer, 2005.
- [36] N. Tsuboi S. Katoh and A.K. Hayashi. Three-dimensional numerical simulation for hydrogen/air detonation: rectangular and diagonal structures. *Proceedings of the Combustion Institute*, 29:2783–2788, 2003.
- [37] M. Berger and J. Olinger. Adaptive mesh refinement for hyperbolic partial differential 410 equations. *Journal of Computational Physics*, 53:484–512, 1984.
- [38] Keitaro Etoa Nobuyuki Tsuboi and A. Koichi Hayashi. Numerical study on three-dimensional C-J detonation waves: detailed propagating mechanism and existence of OH radical. *Proceedings of the Combustion Institute*, 30:1907–1913, 2005.
- [39] D.N. Williams L.Bauwens and E.S. Oran. Detailed structure and propagation of three-dimensional detonations. *Proceedings of the Combustion Institute*, 26:2991–2998, 1997.
- [40] H.S.L. John. Dynamic parameters of gaseous detonations. *Annu. Rev. Fluid Mech.*, 16:311–336, 1984.
- [41] Oran E.S. Weber Jr. J.W. Stefaniw E.I. Lefebvre M.H. and Anderson Jr. J.D. A numerical study of a two-dimensional H₂-O₂-Ar detonation using a detailed chemical reaction model. *Combustion and Flame*, 113:147–163, 1998.